Original Research Article

Ferrite Quantum Dot/Graphene Nanohybrids for Interfacial Tension Reduction: A Reservoir Alteration Wettability for Enhancing Oil Recovery

S.O. Azeez[1], O. Adedokun[2, *], K.O. Suleman[3], A.A. Adewale[2], K.K. Babalola[1], T.T. Adeojo[1], O.F. Adewumi[1], T.A. Adedosu[4], Y.K. Sanusi[2], L.A. Sunmonu[2]

[1]*Department of Physical and Chemical Sciences, Federal University of Health Sciences, Ila-Orangun, Nigeria*
[2]*Department of Pure and Applied Physics, Ladoke Akintola University of Technology, Ogbomoso, Nigeria*
[3]*Department of Physics, School of Basic Sciences, Nigeria Maritime University Okerenkoko, Delta State, Nigeria*
[4]*Department of Pure and Applied Chemistry, Ladoke Akintola University of Technology, Ogbomoso, Nigeria*

Citation S.O. Azeez, O. Adedokun, K.O. Suleman, A.A. Adewale, K.K. Babalola, T.T. Adeojo , O.F. Adewumi, T.A. Adedosu, Y.K. Sanusi, L.A. Sunmonu. Ferrite Quantum Dot/Graphene Nanohybrids for Interfacial Tension Reduction: A Reservoir Alteration Wettability for Enhancing Oil Recovery. *J. Eng. Ind. Res.* **2025**, 6 (4):324-336.

https://doi.org/10.48309/JEIRES.2025.530846.1244

CC BY

Article info:
Submitted: 2025-06-20
Revised: 2025-07-23
Accepted: 2024-08-13
ID: JEIRES-2506-1244

Keywords:
Quantum dot hybrids; Nanofluid; Graphene quantum dots; Rock reservoir; Alteration wettability.

ABSTRACT

This study introduces a new technique that utilizes nanohybrids made from graphene ferrite ($CoFe_2O_4$) quantum dots nanohybrids (G-FQDs). These nanohybrids are produced through a manufacturing process that is both inexpensive and scalable for commercial use. When these FQDs-G nanohybrids are dispersed in a fluid to form nanofluids, they significantly lower the interfacial tension the force at the boundary between oil and water. Reducing this tension helps to improve the displacement of oil in reservoirs, making these nanofluids highly effective for enhanced oil recovery (EOR) technologies. The graphene synthesis involves chemical exfoliation using deionized water, strong acids, and oxidants, while ferrite quantum dots (FQDs) are produced via a hydrothermal method using castor oil plant precursors. The G-FQDs nanohybrids are fabricated using a sol-gel process and characterized using techniques such as XRD, FTIR, and HRTEM. We investigated the mechanism of these nanofluids under reservoir-simulated conditions. The results demonstrate that 0.5-G-FQDs nanofluid optimally modifies wettability in oil-wet carbonate slabs while exhibiting the optimal stability through minimal droplet formation. These nanohybrids significantly reduce interfacial tension, with oil/water IFT dropping from 14.5 mN/m to 1.80 mN/m and n-decane/water IFT, which is a standard hydrocarbon phase that mimics the properties of crude oil decreasing from 46.6 mN/m to 24.3 mN/m. This study confirms the potential of G-FQDs nanohybrids for enhancing EOR efficiency.

***Corresponding Author: Oluwaseun Adedokun** (*oadedokun@lautech.edu.ng*)

Introduction

Several types of nanoparticles (NPs) are abundant and play a critical role in many fields. These materials have emerged from recent advances in science and technology. They are widely used in some areas such as reservoir engineering, catalysis, and biomedical applications [1-4]. Therefore, the long-term use of NPs for other applications is attributed to their unique nanoscale qualities and favorable susceptibility, which differ from ordinary microparticles [5-6]. In reservoir engineering applications, nanoparticles can move freely through the pores of reservoir rocks due to their extremely small size, enabling them to be manipulated or directed by external forces for enhanced performance. Due to their consistence and stability, nanoparticles (NPs) have been effectively utilized to modify reservoir conditions, particularly by altering rock surface wettability and decreasing interfacial tension (IFT) between crude oil and water, leading to enhanced oil recovery [3,7-8]. While silica-based nanomaterials have historically been prominent for this purpose, recent advancements have highlighted metal oxide-based nanomaterials as superior agents for reservoir conditioning [9,10-13].

Nanofluid is a new type of oil displacement agent, typically made by dispersing nanoparticles in a liquid, usually water-based. Compared to traditional chemical oil displacement agents, nanofluids offer several advantages including a high specific surface area, excellent biocompatibility, and improved oil recovery efficiency [14,15-19]. In recent years, scholars have discovered that graphene-based flaky nanomaterials show great promise as oil displacement materials with wide application potential [20]. Graphene oxide (GO) is a key derivative of graphene and represents a new type of two-dimensional carbon nanomaterial. It retains several properties of graphene, such as a large specific surface area, high thermal conductivity, and strong mechanical strength. Additionally, the GO surface contains numerous oxygen-rich functional groups, which make it hydrophilic and easily dispersible in water. Due to these features, GO nanofluids have significant potential to enhance oil recovery [14,21-23]. Core flooding experiments have demonstrated that Fe_2O_3, Al_2O_3, and SiO_2 NPs, when dispersed in propanol, significantly reduce interfacial tension (IFT) from 38.50 mN/m to 2.75, 2.75, and 1.45 mN/m, respectively, leading to enhanced oil recovery [1,3,9-11,16]. Additionally, SiO_2 NPs improve the wettability of quartz rock surfaces, an effect attributed to their hydrophilic nature and influenced by several factors such as ionic composition, salinity, nanoparticle concentration, and interaction time with the rock surface[24].

Yahya et al. [25] used cobalt ferrite nanoparticles as a nanofluid in conjunction with electromagnetic waves. This method yielded a residual oil recovery of 31.58%, significantly higher than the 8.70% recovery when the nanofluid was used without electromagnetic waves. Cobalt ferrite nanoparticles were synthesized via the sol-gel method and characterized by X-ray diffraction (XRD) and electron microscopy, revealing particle sizes around 26–62 nm depending on annealing temperature [26]. Recent research by Rashid et al. [26] has revealed that combining graphene quantum dots (GQDs) with ferrite nanoparticles significantly enhances their dielectric and magnetic properties. These improvements are vital for optimizing oil recovery processes. Specifically, Co-Zn ferrite nanocomposites decorated with GQDs demonstrated superior dielectric and magnetic performance, making them promising candidates for use as contrast agents and in microwave absorption applications [26]. However, a significant research gap exists regarding the systematic design of G-FQD nanohybrids using scalable synthesis methods and their efficacy in modifying reservoir wettability for EOR.

This study shows a new way to make graphene-ferrite quantum dot nanohybrids (G-FQDs). The process involves three main materials: cobalt ferrite ($CoFe_2O_4$), carbon quantum dots, and graphene nanoparticles. These materials are combined step-by-step to create the final nanohybrid. The critical parameters were investigated including nanohybrid size modulation and concentration optimization. The results demonstrated remarkable wettability

alteration, with contact angle of 21.0° (deionized water baseline) and a post-treatment shift to 78.5° water-wet state. This synergistic combination enables precise control over fluid dynamics in porous media, particularly in carbonate reservoirs where traditional surfactants show limited effectiveness.

Experimental

Materials

Ninety-nine percent pure iron (III) chloride hexahydrate ($FeCl_3 \cdot 6H_2O$), sodium hydroxide (NaOH), and ethanol (C_2H_5OH) were commercially sourced. These reagents were utilized without any additional purification, followed by drying in an oven. A 0.22 µm filter paper was utilized to filter the extract during experiments. Throughout the study, only deionized distilled water was employed for all procedures. Other materials included hot plate, gloves, 10 ml syringe, water disperser, spatula, Petri dish, forceps, aluminum foil, plastic weighing trays, the N-decane was sourced from Merck Co., Germany. Carbonate and sandstone rock samples were collected from outcrops of two reservoirs located in the eastern region of Nigeria.

Collection and identification

Castor oil plant specimens were collected from LAUTECH botanical garden, Ogbomosho, Nigeria. The collected green plant material was processed to extract the necessary substances and subsequently stored in a refrigerator for future use. Prior to any experimental procedures, the glassware was cleaned with deionized water, followed by ethanol to ensure thorough decontamination of any potential organic contaminants.

Preparation Ricinus communis plant extract

The leaves of Ricinus communis were thoroughly washed with deionized water to eliminate any contaminants before being air-dried to remove excess moisture. 50 g of the dried leaves were then ground using a mortar and pestle to create a fine powder. This powdered leaf material was subsequently heated in 100 mL of deionized water for approximately one hour at 80 °C, until the water showed a green color. Afterward, the solid residue was discarded, and the resulting plant extract was collected as a filtrate in a beaker using 0.22 µm Whatman filter paper. The aqueous extract was then stored in a refrigerator until needed for further applications.

Synthesis of carbon quantum dots (CQDS)

50 mL of Ricinus communis extract were placed into a Teflon-lined stainless-steel autoclave for hydrothermal treatment at 120 to 280 °C for 12 h. After the reaction, the autoclave was naturally cooled to ambient temperature. During this hydrothermal process, the solution was changed to a dark brown color, indicating the C-dot formation. These carbon dots were purified to remove the larger nanoparticles by 2 µm filter paper. The microstructure and particle size distribution of the C-dots were determined using high-resolution transmission electron microscopy (HRTEM) and dynamic light scattering. The synthesis method is in line with that suggested by Hoan et al. [13].

Synthesis of FQD nanocomposite

The FQD nanocomposite was synthesized using hydrothermal method with a weight ratio of 2:1. Specifically, 2 mmol (0.02 g) of $CoFe_2O_4$ and 1 mmol (0.01 g) of gelatin-CQDs were mixed in 10 mL of ethanol for 15 minutes until a homogeneous dispersion was achieved. The resulting solution was then heated to 70 °C in an oil bath under an argon atmosphere while being stirred magnetically for 4 hours. After the reaction, the brown precipitate was separated using a strong external magnet, washed alternately with distilled water and ethanol in a 2:1 ratio, and dried overnight in an oven at 40 °C [27].

Synthesis of graphene oxide (GO)

Graphene oxide was synthesized from graphite pencil lead through a modified version of Hummer's method .2 g of finely powdered graphite pencil lead were placed in 50 ml of H_2SO_4, and the solution was thoroughly stirred

with a magnetic stirrer for 60 minutes under an ice bath. Thereafter, 7 g of $KMNO_4$ was slowly added to the mixture during the stirring process. Afterward, the mixture was transferred to an oil bath and the mixture was stirred constantly at 500 revolutions per minute (RPM) for 40 minutes. Subsequently, 150 mL of RO water was added to the solution and stirred the mixture continually for about 20 minutes. Next, 400 mL was added, followed by the slow addition of H_2O_2 to eliminate the residue. A change in color was observed by visual inspection from brown to yellowish. The suspension was filtered and washed with 250 mL of dilute HCl (1:10). The resulting solution was dried, followed by adding 500 ml of water. The GO solution was washed repeatedly to remove all residual salts and acids. The neutralized GO solution was stirred overnight, followed by sonication process to exfoliate the graphite oxide into graphene oxide. The GO dispersion was stored for the reduction process. GO and Ricinus communis leaf extract were mixed together by varying the GO at different ratios of 1:1, 1:2, and 1:4 under vigorous stirring 500 RPM for 8 h. Subsequently, the mixtures were washed with deionized water and sonicated for 30 min. This treatment was repeated several times until a clear solution was obtained, and then the ingredients were dried in a vacuum oven.

Synthesis of G-FQDs nanohybrids

Typically, G-FQDs nanohybrids are prepared by a sol-gel process with a weight ratio of 2:1. 2 mmol (0.02 mg) of ferrite QDs and 1 Mmol (0.01 mg) of graphene were poured into 10 ml of ethanol and completely mixed for 15 min until dispersion. Thereafter, the solution was heated at 80 °C in an oil bath and thoroughly combined under argon gas and a magnetic stirrer for 5 h. The resultant solution was dried in an oven overnight at 40 °C.

Preparation and characterization of cores and slabs

A core plugging system was utilized to prepare core plugs for core flooding experiments. Initially, a cutter was used to trim both ends of the sandstone and carbonate cores. For contact angle measurements, standard 1-inch diameter rock cores were sliced into several pieces with a thickness of 0.2 cm and then polished following a standard procedure detailed in the literature [28,29].

Contact angle and IFT measurement

The slabs were primarily aged in oil at 60 °C and 1 atm for 24 h, and then dried in an oven for 6 h at 60 °C [30]. Consequently, the oil-infused slabs were immersed in nanofluids and deionized water (DW) for 72 h. The oil contact angle, which is the angle between the submerged slab surface and the surrounding aqueous fluid, was recorded using a camera and subsequently analyzed with ImageJ plugins (software). When the oil contact angle is less than 90°, approximately 90°, or more than 90°, the wettability of the system is classified as oil-wet, intermediate-wet, or water-wet, respectively [7]. The experiments have demonstrated that altering the wettability of porous media from oil-wet to water-wet significantly enhances oil recovery [15].

The interfacial tension (IFT) between oil/water nanofluids and n-decane/water nanofluids was measured using an IFT-400 tensiometer at four different nanofluid concentrations such as 0 mg/mL (neat deionized water), 0.2 mg/mL, 0.4 mg/mL, and 0.6 mg/mL of nanoparticles (NPs). IFT measurements were conducted based on the pendant drop method, as shown in Figure 1. In the procedure, the quartz chamber was initially filled with either water or the respective nanofluid, and an oil droplet was formed using a needle. Images captured during this process were then analyzed to determine the IFT values. The pendant drop method calculates the oil/water IFT using two experimental parameters: the equatorial diameter (de) and the diameter (ds) measured at a distance of de from the top of the oil droplet. The IFT is computed using Equation 1 [10].

$$IFT = \frac{\Delta \rho g d_e^2}{H} \quad (1)$$

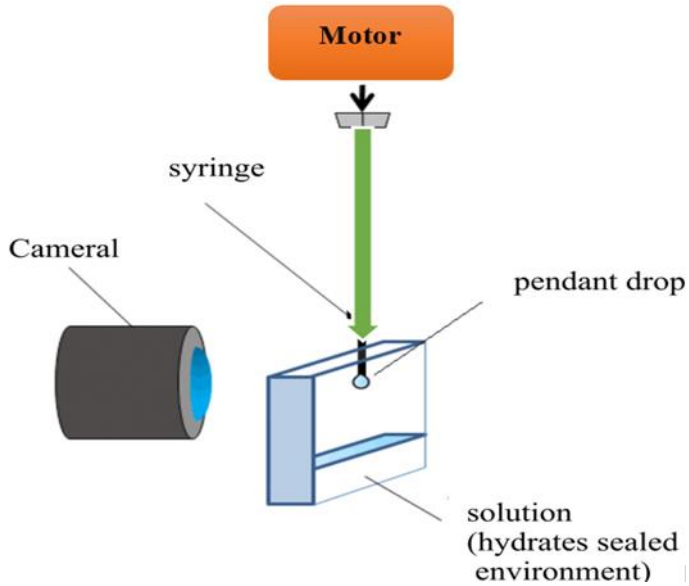

Figure 1: Schematic diagram of pendant drop.

Characterization of prepared G-FQDs nanohybrid

The crystalline structures and other structural characteristics of the G-FQDs nanohybrid were analyzed using a Rigaku Smartlab X-ray diffractometer, with an X-ray generator operating at 40 kV and 30 mA for X-ray powder diffraction. To investigate its chemical composition and functional groups, Fourier Transform Infrared (FTIR) spectroscopy was conducted using a Perkin Elmer FTIR spectrometer over the range of 4000 to 400 cm^{-1}. Additionally, High-Resolution Transmission Electron Microscopy (HRTEM) was employed to examine the nanoscale morphology, including size distribution and agglomeration of G-FCQDs within the graphene matrix. Finally, the contact angle and interfacial tension (IFT) were measured using optical tensiometers after subjecting the samples to hydrothermal carbonization for 0.5, 1, 1.5, and 2 hours.

Elmer FTIR spectrometer over the range of 4000 to 400 cm^{-1}. Additionally, High-Resolution Transmission Electron Microscopy (HRTEM) was employed to examine the nanoscale morphology, including size distribution and agglomeration of G-FCQDs within the graphene matrix. Finally, the contact angle and interfacial tension (IFT) were measured using optical tensiometers after subjecting the samples to hydrothermal carbonization for 0.5, 1, 1.5, and 2 hours.

Results and Discussion

FTIR analysis

The FT-IR spectra for G, FQDs and G-FQDs nanocomposite are depicted in Figure 2. The spectra exhibit a broad absorption band between 3300 and 4450 cm^{-1}, along with distinct peaks in the 1400-1649 cm^{-1} range, which likely correspond to the stretching vibrations of O-H groups from water molecules adsorbed on the catalyst surface. For G, a peak at 590 cm^{-1} is attributed to the stretched model of O-H bond vibrations. Additionally, a peak at 1048 cm^{-1} may indicate the stretching vibration of Co in a metal-organic chelate, formed during the synthesis of $CoFe_2O_4$ due to the chelation of ethylene glycol and metal ions. The peaks in the 1380-1390 cm^{-1} range could be related to C-O-H formation in the in-plane band, resulting from the interaction between $CoFe_2O_4$ and G. Furthermore, the absorption peak at 575 cm^{-1} likely reflects Fe-O and Co-O bond vibrations within $CoFe_2O_4$. The comparative analysis of peaks between the G-FQDs composite and FQDs supports the successful synthesis of the composite material.

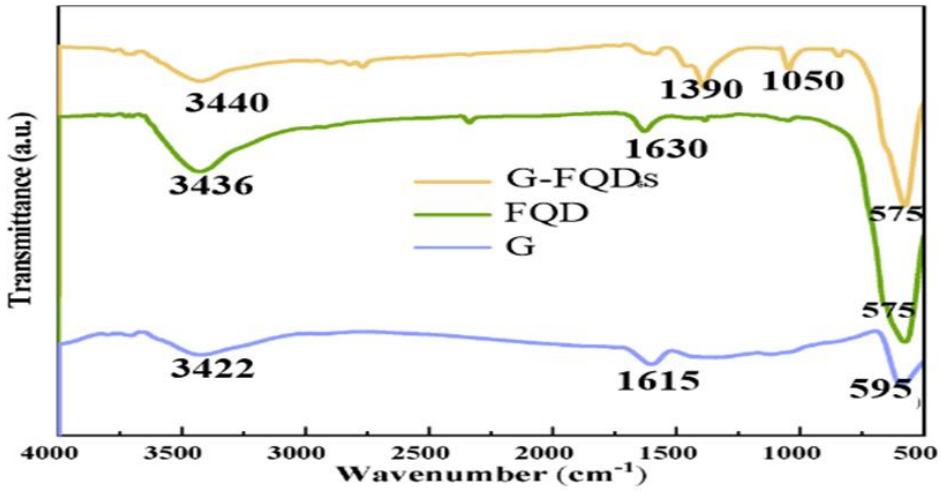

Figure 2: FTIR analysis of G-FQDs, FQDs, and graphene.

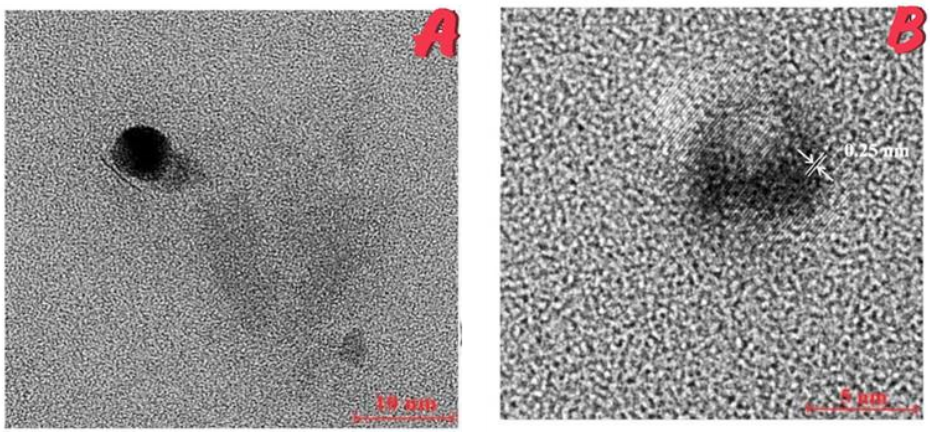

Figure 3: HRTEM analysis of G-FQDs nanohybrid

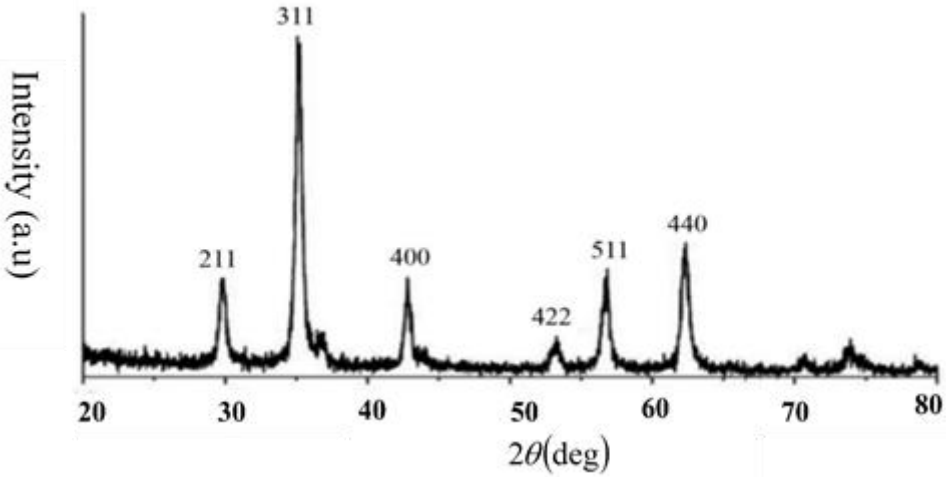

Figure 4: XRD analysis of G-FQDs nanohybrid.

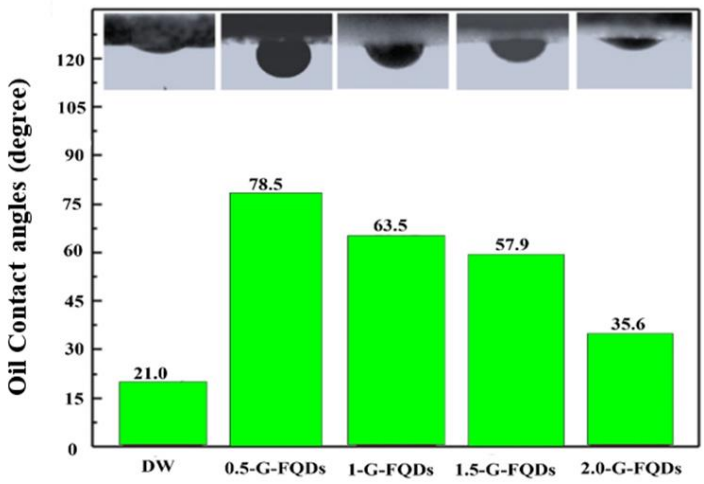

Figure 5: Contact angle after the treatment with carbonate rock of different nanofluids.

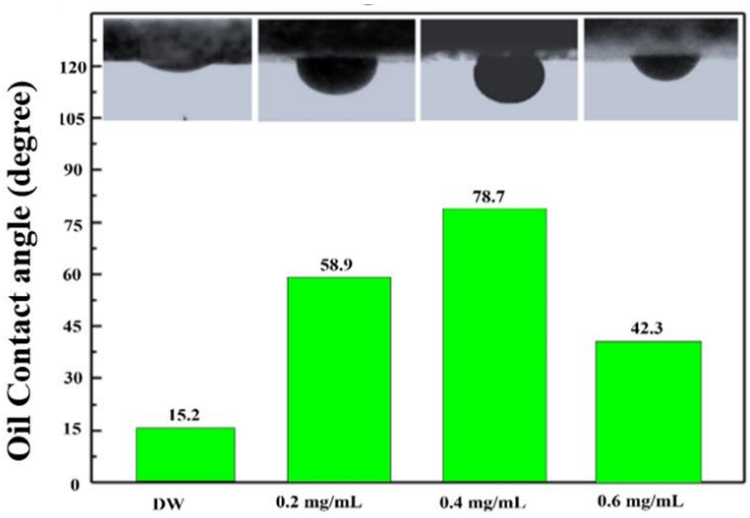

Figure 6: Oil contact angles after treatment of carbonate rocks with different concentrations of 0.5-G-FQDs.

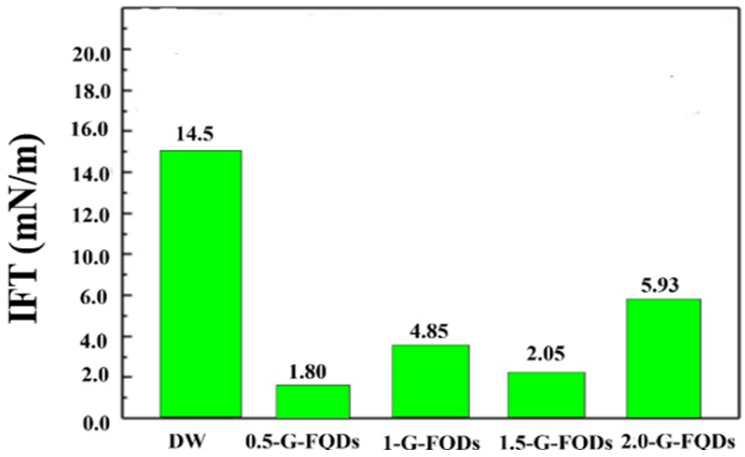

Figure 7: IFT alterations between oil and fluids (water and nanofluids).

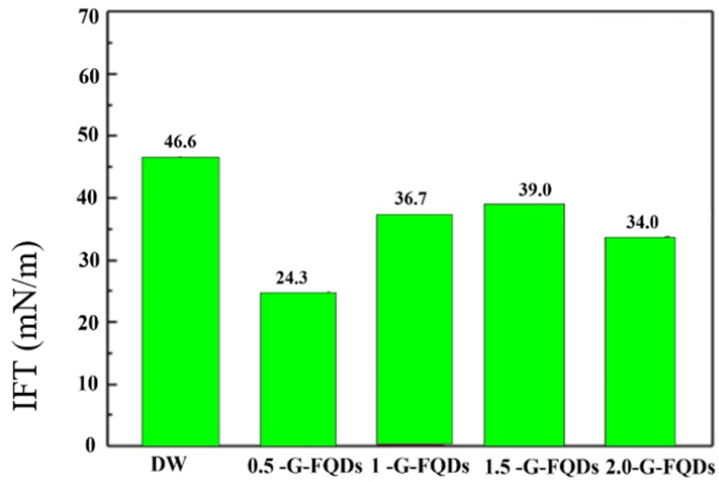

Figure 8: IFT alterations between n-decane and fluids (water and nanofluids).

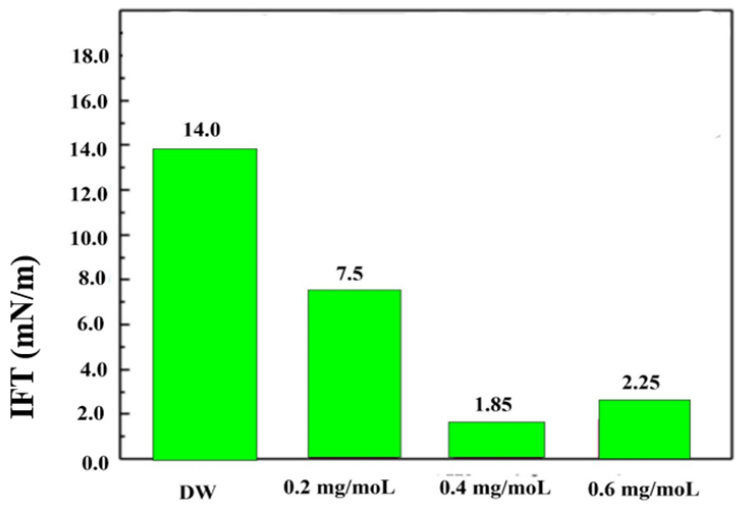

Figure 9: Alterations between oil and nanofluids with different concentrations of 0.5-G-FQDs.

HRTEM analysis

High-Resolution Transmission Electron Microscopy (HRTEM) is advanced imaging technique allows us to visualize materials at the atomic level, providing critical insights into their structural and functional properties. The G-FQDs images, along with the droplet size distribution, are presented in Figure 3. The HRTEM images reveal that the average droplet sizes of G-FQDs, determined using Digimizer image analysis software, range from 5 to 10 nm. Additionally, the droplets are uniformly dispersed in solution without any signs of agglomeration. The absence of agglomeration suggests that the nanoparticles are evenly distributed. This consistency is essential for maximizing the surface area available for interactions with oil and enhancing the efficiency of recovery processes. When particles are well-dispersed, they can more effectively interact with the oil, leading to improved recovery rates.

XRD analysis

The G-FQDs. composite was characterized using Rigaku Smartlab X-ray diffractometer. The x-ray diffraction analysis pattern of the G-FQDs in powder form is demonstrated in Figure 5. The analysis was conducted for angles ranging from 20º to 80º. Five noticeable diffraction peaks

occurred at Bragg's angles 30°, 43°, 53°, 58°, and 63°corresponding to the planes (211), (400), (422), (511), and (440), respectively. The XRD spectra identify the mineral composition of rocks and soils and crystalline structure of G-FQDs, which is crucial in understanding reservoir properties and potential oil-bearing formations. The three as-prepared composites exhibit a strong diffraction peak around 35º which corresponds to the most abundant mineral or the phase in the reservoir rock, potentially impacting the oil migration and accumulation.

Alternation of wettability

Wettability alteration is a critical enhanced oil recovery (EOR) technique that modifies reservoir rock surfaces to improve oil displacement efficiency. By shifting rock wettability from oil-wet to water-wet conditions, this method decreases residual oil saturation and enhances hydrocarbon mobility through capillary forces and imbibition mechanisms [31].

Effect of G-FQDs size

Contact angle measurements were conducted to determine the flow rate of oil in the presence of diverse nanofluids, including deionized water (DW) as a control. As demonstrated in Figure 4, the contact angle of oil with DW was measured at 21.0°, indicating that the carbonate slabs exhibited oil-wet conditions. Notably, the 0.5-G-FQDs introduction raised the oil contact angle significantly from 21.0° to 78.5°, marking the most substantial change in wettability observed among all G-FQDs tested at different sizes. These data suggest a shift in the wettability of the carbonate slabs to a water-wet state due to the effect of 0.5-G-FQDs. Additionally, larger G-FQDs resulted in oil contact angles that approached those observed under the initial oil-wet condition (oil/water without G-FQDs). Smaller G-FQDs were more effective in altering surface properties, as their size allowed them to penetrate and interact more effectively with the rock surface and oil droplets, resulting in higher disjoining pressures [3]. Structural disjoining pressure is a mechanism reported in several studies that explains changes in the wettability of oil-wet rocks in the presence of nanoparticles (NPs) [30,32-33]. It refers to the pressure needed to overcome the adhesive forces between the oil (fluid) and the solid surface (rock slabs), leading to the oil detachment from the surface. According to this mechanism, NPs form a wedge-shaped film at the oil/water/rock interface. The size and concentration of these nanoparticles are crucial factors affecting the magnitude of the surface disjoining pressure. When NP size decreases, Brownian motion effects become more pronounced, and increasing NP concentration enhances the repulsive forces between particles. This results in a higher structural disjoining pressure, contributing to better wettability modification [5].

Effect of G-FQDs concentration

The 0.5-G-FQDs exhibited the most optimal performance among the four G-FQDs in altering the wettability of oil-wet carbonate slabs. Consequently, additional contact angle measurements were conducted on 0.5-G-FQDs samples at concentrations of 0.2, 0.4, and 0.6 mg/mL to investigate how G-FQDs concentration influences the wettability of these carbonate slabs. The results in Figure 6 indicate an optimal G-FQDs concentration of 0.4 mg/mL; below this level, the oil contact angle on the carbonate slabs decreased, while above it, the G-FQDs effectiveness in altering wettability diminished. This aligns with existing results [11]. As the G-FQDs concentration approaches the optimal level of 0.4 mg/mL, the number of G-FQDs between the carbonate rock and the oil droplet increases, enhancing repulsive forces and structural disjoining pressure. Therefore, the oil contact angle rises. However, at higher G-FQDs concentrations, the NPs stability in the base fluid and wedge film is compromised due to increased charge density in the wedge layer [34]. As a result, the NPs ability to modify the wettability of carbonate slabs is diminished. Additionally, concentrations exceeding a certain threshold led to agglomeration, preventing the particles from adequately covering the rock surface and altering its wettability.

IFT reduction

Interfacial tension (IFT) plays a crucial role in enhanced oil recovery (EOR) by affecting the mobilization of trapped oil within reservoir rocks. High IFT between oil and water phases creates strong capillary forces that prevent oil from being displaced by injected fluids. Reducing IFT is therefore a key strategy for increasing oil recovery, especially in oil-wet formations where residual oil is strongly retained [16].

Effect of G-FQDs size

The interfacial tension (IFT) between oil and water is a crucial factor in enhanced oil recovery (EOR), as lower IFT values generally facilitate increased oil extraction. The effect of the size of graphene/ferrite quantum dots (G-FQDs) on oil/water IFT and N-decane/water IFT was investigated. Similar to the wettability results presented in Figures 7 and 8, the 0.5-G-FQDs application led to a significant reduction in oil/water IFT, decreasing from 14.5 mN/m to 1.80 mN/m, and a reduction in N-decan/water IFT, which fell from 46.6 mN/m to 24.3 mN/m. These findings align with the existing literature [21]. The G-FQDs with the smallest sizes yielded the lowest IFT values (1.80 mN/m in oil/water systems, and 24.3 mN/m in N-decane/water systems), while those with the largest sizes resulted in the highest IFT values. Generally, our measurements show that larger G-FQDs promoted larger IFT. Similar to how surfactants function, nanoparticles (NPs) gather at the oil-water boundary and lower interfacial tension (IFT). This IFT reduction is more noticeable with smaller NPs because a higher quantity can pack into the interface. Furthermore, smaller NPs provide a larger surface area for contact with the oil phase, enhancing asphaltene adsorption onto the NP surface. This adsorption hinders asphaltene molecules from depositing at the oil-water interface [35]. These factors explain why the smallest 0.5-G-FQDs in this study resulted in a greater decrease in IFT compared to the larger G-FQDs. Based on their superior IFT reduction, the 0.5-G-FQDs were selected for further investigation into the effect of their concentration (0.2, 0.4, and 0.6 mg/mL) on IFT.

The G-FQDs concentration has a complex effect on oil/water interfacial tension (IFT). The small size of the 0.5-G-FQDs facilitates their accumulation at the oil/water interface. As the concentration increases from 0.2 mg/mL to 0.4 mg/mL, IFT is significantly reduced, as demonstrated in Figure 9, likely due to increased particle packing at the interface. However, further increases to 0.6 mg/mL lead to the G-FQDs aggregation in the base fluid, decreasing stability and resulting in a diminished IFT reduction, a trend observed in other research [19]. It is also possible that at these high concentrations, the G-FQDs form an over-packed, rigid layer at the interface. This tightly packed layer could increase cohesive forces between the oil and water, leading to a counterintuitive increase in IFT [34]. These findings suggest that the optimal type and concentration of G-FQDs—specifically 0.5-G-FQDs at 0.4 mg/mL—significantly reduced the interfacial tension (IFT) between oil and water, lowering it from 14.00 mN/m (deionized water only) to 1.85 mN/m. Wettability and IFT measurements confirm that 0.5-G-FQDs are the most effective in altering the interfacial properties of both the oil/water/rock and oil/water interfaces, with 0.4 mg/mL identified as the optimal concentration for this type of nanoparticles.

Conclusion

G-FQD dispersions of varying sizes were synthesized by adjusting the hydrothermal reaction time in water and subsequently used for flooding sandstone and carbonate cores in enhanced oil recovery (EOR) applications. Longer reaction periods produced larger G-FQDs. Wettability tests on carbonate rocks revealed that nanofluids containing smaller G-FQDs more effectively modified wettability, with 0.5-G-FQDs delivering the most significant improvements. Concentration-dependent studies identified 0.4 mg/mL as the optimal concentration of 0.5-G-FQDs among the tested samples, while the G-FQDs nanofluids showed no effect on sandstone wettability. Additionally, the ability of the nanofluids to decrease oil/water and n-heptane/water interfacial tensions increased with decreasing G-FQDs size.

Notably, the 0.5-G-FQDs nanofluid at 0.4 mg/mL concentration achieved the greatest reduction in interfacial tension, lowering the oil/water IFT from 14.5 mN/m to 1.80 mN/m, and the n-heptane/water IFT from 46.6 mN/m to 24.3 mN/m. The 0.5-G-FQDs nanofluid induced a dramatic wettability shift in carbonate slabs: the contact angle increased from 21.0° to 78.5°. These results clearly reveal that the introduction of prepared nanofluid effectively altered the wettability of carbonate slabs and sand stone stones, transforming their surfaces from oil-wet to a more water-wet state.

ORCID

S.O. Azeez: 0000-0001-5737-1388
O. Adedokun: 0000-0002-7947-8415
K.O. Suleman: 0000-0002-9103-1974
A.A. Adewale: 0000-0001-8768-3876
K.K. Babalola: 0009-0001-1982-6043
T.T. Adeojo: 0009-0002-2050-8787
O.F. Adewumi: *0000-0003-1448-5291*
T.A. Adedosu: 0000-0002-3892-3041
Y.K. Sanusi: 0000-0001-6259-1166
L.A. Sunmonu: 0000-0002-4305-8363

Reference

[1] A. Agi, R. Junin, A. Gbadamosi, M. Manan, M. Z. Jaafar, M.O. Abdullah, A. Arsad, N.B. Azli, M. Abdurrahman, F. Yakasai, Comparing natural and synthetic polymeric nanofluids in a mid-permeability sandstone reservoir condition, *Journal of Molecular Liquids*, **2020**, *317*. [Crossref], [Google Scholar], [Publisher]

[2] M. Ashraf, I. Khan, M. Usman, A. Khan, S.S. Shah, A.Z. Khan, K. Saeed, M. Yaseen, M.F. Ehsan, M. N. Tahir, N. Ullah, Hematite and Magnetite Nanostructures for Green and Sustainable Energy Harnessing and Environmental Pollution Control: A Review, *Chemical Research in Toxicology*, **2020**, *33*, 1292–1311. [Crossref], [Google Scholar], [Publisher]

[3] S. Bagherpour, A. Rashidi, S.H. Mousavi, N. Izadi, E. Hamidpour, Experimental investigation of carboxylate-alumoxane nanoparticles for the enhanced oil recovery performance, *Colloids and Surfaces A: Physicochemical and Engineering Aspects*, **2019**, *563*, 37–49. [Crossref], [Google Scholar], [Publisher]

[4] I.A. Baragau, Z. Lu, N.P. Power, D.J. Morgan, J. Bowen, P. Diaz, S. Kellici, Continuous hydrothermal flow synthesis of S-functionalised carbon quantum dots for enhanced oil recovery, *Chemical Engineering Journal*, **2021**, *405*, 126631. [Crossref], [Google Scholar], [Publisher]

[5] A. Bera, S. Shah, M. Shah, J. Agarwal, R.K. Vij, Mechanistic study on silica nanoparticles-assisted guar gum polymer flooding for enhanced oil recovery in sandstone reservoirs, *Colloids and Surfaces A: Physicochemical and Engineering Aspects*, **2020**, *598*, 124833. [Crossref], [Google Scholar], [Publisher]

[6] K.P. Dahkaee, M.T. Sadeghi, Z. Fakhroueian, P. Esmaeilzadeh, Effect of NiO/SiO2 nanofluids on the ultra interfacial tension reduction between heavy oil and aqueous solution and their use for wettability alteration of carbonate rocks, *Journal of Petroleum Science and Engineering*, **2019**, *176*, 11–26. [Crossref], [Google Scholar], [Publisher]

[7] A.D. dos Santos Francisco, K.C.B. Maia, L. de Almeida Cavadas, F.M. Eler, D. Grasseschi, P. Couto, R.S.V. Nascimento, Wettability alteration of oil-wet carbonate rocks by chitosan derivatives for application in enhanced oil recovery ii: High-temperature and high-pressure conditions—core flooding tests, *Journal of Applied Polymer Science*, **2024**, *141*, e55372. [Crossref], [Google Scholar], [Publisher]

[8] K. Guo, H. Li, Z. Yu, Metallic nanoparticles for enhanced heavy oil recovery: Promises and challenges, *Energy Procedia*, **2015**, 75, 2046–2051. [Crossref], [Google Scholar], [Publisher]

[9] J.L. Gómez-Delgado, J.J. Rodriguez-Molina, J.C. Perez-Angulo, N. Santos-Santos, E. Mejía-Ospino, Evaluation of the wettability alteration on sandstone rock by graphene oxide adsorption, *Emergent Materials*, **2024**, *7*, 2045–2054. [Google Scholar], [Publisher]

[10] H. Soleimani, N. Yahya, M. Baig, L. Khodapanah, M. Sabet, M. Burda, A. Oechsner, M. Awang, Synthesis of carbon nanotubes for oil-water interfacial tension reduction, *Oil and Gas Res*, **2015**, *1*, 1000104. [Crossref], [Google Scholar], [Publisher]

[11] S.Habibi, A. Jafari, Z. Fakhroueian, Application of novel functionalized al2o3/silica by organosiloxane and amine reagents for

enhanced oil recovery, *Applied Nanoscience*, **2020**, *10*, 2085–2100. [Google Scholar], [Publisher]
[12] Y.M. Hassan, B.H. Guan, L.K. Chuan, A. Halilu, M. Adil, A.A. Adam, B.A. Abdulkadir, Interfacial tension and wettability of hybridized znofe2o3/sio2 based nanofluid under electromagnetic field inducement, *Journal of Petroleum Science and Engineering*, **2022**, *211*, 110184. [Crossref], [Google Scholar], [Publisher]
[13] B.T.Hoan, P.D. Tam, V.H. Pham, Green synthesis of highly luminescent carbon quantum dots from lemon juice, *Journal of Nanotechnology*, **2019**, 2852816. [Crossref], [Google Scholar], [Publisher]
[14] R.Hosny, A. Zahran, A. Abotaleb, M. Ramzi, M.F. Mubarak, M.A. Zayed, A.E. Shahawy, M.F. Hussein, Nanotechnology impact on chemical-enhanced oil recovery: A review and bibliometric analysis of recent developments, *ACS omega*, **2023**, *8*, 46325–46345. [Crossref], [Google Scholar], [Publisher]
[15] E. Hosseini, N. Hosseini, M. Sarmadivaleh, Wettability modification effects on relative permeability end-points: Comparative analysis of surfactant agents for enhanced oil recovery, *Petroleum Research*, **2024**, *9*, 206–218. [Crossref], [Google Scholar], [Publisher]
[16] H. Imuetinyan, A. Agi, A. Gbadamosi, R. Junin, J. Oseh, Oil-water interfacial tension, wettability alteration and foaming studies of natural surfactant extracted from vernonia amygdalina, *Petroleum Research*, **2022**, *7*, 350–356. [Crossref], [Google Scholar], [Publisher]
[17] N. Izadi, B. Nasernejad, Newly engineered alumina quantum dot-based nanofluid in enhanced oil recovery at reservoir conditions, *Scientific reports*, **2022**, *12*, 9505. [Crossref], [Google Scholar], [Publisher]
[18] E. Jafarbeigi, F. Salimi, E. Kamari, M. Mansouri, Effects of modified graphene oxide (go) nanofluid on wettability and ift changes: Experimental study for eor applications, *Petroleum Science*, **2022**, *19*, 1779–1792. [Crossref], [Google Scholar], [Publisher]
[19] A. Khalilnezhad, H. Rezvani, P. Ganji, Y. Kazemzadeh, A complete experimental study of oil/water interfacial properties in the presence of tio2 nanoparticles and different ions, *Oil & Gas Science and Technology–Revue d'IFP Energies Nouvelles*, **2019**, *74*, 39. [Crossref], [Google Scholar], [Publisher]
[20] G. Kumar, U.S. Behera, E. Mani, J.S. Sangwai, Engineering the wettability alteration of sandstone using surfactant-assisted functional silica nanofluids in low-salinity seawater for enhanced oil recovery, *ACS Engineering Au*, **2022**, *2*, 421–435. [Crossref], [Google Scholar], [Publisher]
[21] K.C. Lee, Z.A. Bin Saipolbahri, H. Soleimani, H.M. Zaid, B.H. Guan, D.L.C. Ching, Effect of zinc oxide nanoparticle sizes on viscosity of nanofluid for application in enhanced oil recovery, *Journal of Nano Research*, **2016**, *38*, 36–39. [Crossref], [Google Scholar], [Publisher]
[22] A.G. Leonel, A.A. Mansur, H.S. Mansur, Advanced functional nanostructures based on magnetic iron oxide nanomaterials for water remediation: A review, *Water research*, **2021**, *190*, 116693. [Crossref], [Google Scholar], [Publisher]
[23] L. Liang, S. Meng, J. Tao, J. Li, X. Wang, J. Guan, H. Fu, C. Dai, H. Liu, Preparation and application of modified carbon black nanofluid as a novel flooding system in ultralow permeability reservoirs, *Journal of Molecular Liquids*, **2023**, *383*, 122099. [Crossref], [Google Scholar], [Publisher]
[24] T. Liang, J.R. Hou, M. Qu, J.X. Xi, I. Raj, Application of nanomaterial for enhanced oil recovery, *Petroleum Science*, **2022**, *19*, 882–899. [Crossref], [Google Scholar], [Publisher]
[25] K. Liao, Z. Ren, L. Fu, F. Peng, L. Jiang, W. Gu, X. Zhang, J. Bai, Y. He, Effects of surfactants on dispersibility of graphene oxide dispersion and their potential application for enhanced oil recovery, *Journal of Petroleum Science and Engineering*, **2022**, *213*, 110372. [Crossref], [Google Scholar], [Publisher]
[26] R. Liu, Y. Liu, S. Yu, Y. Liu, H. Zhang, L. Zhang, Y. Huang, Y. Liu, X. Wang, Experimental and molecular dynamic studies of amphiphilic graphene oxide for promising nanofluid flooding, *Fuel*, **2022**, 330, 125567. [Crossref], [Google Scholar], [Publisher]
[27] S. Naghash-Hamed, N. Arsalani, S.B. Mousavi, The catalytic performance of cufe2o4@ cqd nanocomposite as a high-perform heterogeneous nanocatalyst in nitroaniline

group reduction, *Scientific reports*, **2023**, *13*, 3329. [Google Scholar], [Publisher]
[28] O. Massarweh, A.S. Abushaikha, The use of surfactants in enhanced oil recovery: A review of recent advances, *Energy Reports*, **2020**, *6*, 3150–3178. [Crossref], [Google Scholar], [Publisher]
[29] M. Mirzavandi, J.A. Ali, A.K. Manshad, B. Majeed, B.S. Mahmood, A.H. Mohammadi, S. Iglauer, A. Keshavarz, Performance evaluation of silica–graphene quantum dots for enhanced oil recovery from carbonate reservoirs, *Energy & Fuels*, **2023**, *37*, 955–964. [Crossref], [Google Scholar], [Publisher]
[30] F. Sagala, A. Hethnawi, N.N. Nassar, Hydroxyl-functionalized silicate-based nanofluids for enhanced oil recovery, *Fuel*, **2020**, *269*. [Crossref], [Google Scholar], [Publisher]
[31] R.Q.M. Nouqabi, G. Zargar, M.A. Takassi, S. Moradi, Wettability alteration in enhanced oil recovery process using new amphoteric and cationic surfactants, *Bioscience Biotechnology Research Communications*, **2017**, 10, 704–709. [Crossref], [Google Scholar], [Publisher]
[32] S. Rashid, S. Perveen, S. Hafeez, S. uddin Asad, M.Z. Khan, F. Azad, Graphene quantum dots (GQDs) decorated Co-Zn ferrite: Structural, morphological, dielectric, and magnetic properties, *Journal of Magnetism and Magnetic Materials*, **2023**, *570*. [Crossref], [Google Scholar], [Publisher]
[33] S. Sakthivel, X. Zhou, E.P. Giannelis, M.Y. Kanj, Carbon nanodots for enhanced oil recovery in carbonate reservoirs, *Energy Reports*, **2021**, *7*, 8943–8959. [Crossref], [Google Scholar], [Publisher]
[34] D. Panahpoori, H. Rezvani, R. Parsaei, M. Riazi, A pore-scale study on improving CTAB foam stability in heavy crude oil–water system using TiO2 nanoparticles, *Journal of Petroleum Science and Engineering*, **2019**, *183*. [Crossref], [Google Scholar], [Publisher]
[35] I. Nowrouzi, A.K. Manshad, A.H. Mohammadi, Effects of TiO2, MgO, and γ-Al2O3 nano-particles in carbonated water on water-oil interfacial tension (IFT) reduction in chemical enhanced oil recovery (CEOR) process, *J. Mol. Liq.,* **2019**, 292, 111348. [Crossref], [Google Scholar], [Publisher]

Copyright © 2025 by authors and SPC (Sami Publishing Company) + is an open access article distributed under the Creative Commons Attribution License(CC BY). which permits unrestricted use, distribution, and reproduction in any medium, provided the original work is properly cited.